

A Spectroscopic and Photometric Study of the Metal-Poor, Pulsating, Post-AGB Binary HD 46703

Bruce J. Hrivnak^{1,2}, Hans Van Winckel³, Maarten Reyniers^{3,4}, David Bohlender⁵,
Christoffel Waelkens³, Wenxian Lu¹

ABSTRACT

The metal-poor post-AGB star HD 46703 is shown to be a single-line spectroscopic binary with a period of 600 days, a high velocity of -94 km s^{-1} , and an orbital eccentricity of 0.3. Light curve studies show that it also pulsates with a period of 29 days. High-resolution, high signal-to-noise spectra were used for a new abundance study. The atmospheric model determined is $T_{eff} = 6250 \text{ K}$, $\log g = 1.0$, $V_t = 3.0 \text{ km s}^{-1}$, and a metal abundance of $[M/H] = -1.5$. A low carbon abundance and lack of s-process element enhancement indicate that the star has not experienced third dredge-up on the AGB. The sulfur and zinc abundances are high compared with iron, and the chemical abundances show a clear anti-correlation with condensation temperature. The abundance depletion pattern is similar to that seen in other post-AGB binaries, and, like them, is attributed to the chemical fractionation of refractory elements onto dust stored in a circumbinary disk and the re-accretion of volatiles in the stellar atmosphere. The infrared excess is small but the excess energy distribution is very similar to what can be expected from a disk. HD 46703 joins the growing list of depleted, post-AGB stars which are likely surrounded by a dusty and stable circumbinary disk.

¹Department of Physics and Astronomy, Valparaiso University, Valparaiso, IN 46383; Bruce.Hrivnak@valpo.edu, Wen.Lu@valpo.edu

²Guest Investigator, Dominion Astrophysical Observatory, Herzberg Institute of Astrophysics, National Research Council of Canada

³Instituut voor Sterrenkunde, K.U.Leuven University, 3001 Leuven (Heverlee) Belgium; Hans.VanWinckel@ster.kuleuven.be

⁴Now at KMI, Department Waarnemingen, Ringlaan 3, 1180 Brussels, Belgium

⁵Dominion Astrophysical Observatory, Herzberg Institute of Astrophysics, National Research Council of Canada; David.Bohlender@nrc-cnrc.gc.ca

Subject headings: stars: abundances – stars: AGB and post-AGB – binaries: spectroscopic – stars: chemically peculiar – stars: individual (HD 46703)

1. INTRODUCTION

During the past decennia, it has been realized that post-AGB stars are chemically much more diverse than anticipated. In the canonical picture, the photospheric content of a post-AGB star is the end-product of the chemical enrichment induced by the thermal pulses of AGB stars, and as such post-AGB stars are ideal tracers for the 3rd dredge-up nucleosynthesis. Some objects are the most s-process enriched objects known to date (e.g., Van Winckel 2003, and references therein), while others are not enriched at all. This dichotomy is very strict, in the sense that mildly enhanced objects are not often observed (Van Winckel 2003, and references therein). For the moment it is not clear whether this dichotomy is caused by a selection effect, or if it is the result of two different evolutionary channels.

In this study, we focus on HD 46703. More than 20 years ago, Bond and Luck drew particular attention to HD 46703 with their abundance studies (Luck & Bond 1984; Bond & Luck 1987). They found the object to be iron-poor, $[\text{Fe}/\text{H}] = -1.6$, but relatively overabundant in carbon ($[\text{C}/\text{Fe}] = +1.0$), nitrogen ($[\text{N}/\text{Fe}] = +1.8$), and oxygen ($[\text{O}/\text{Fe}] = +1.1$) and underabundant in s-process elements (Y,Zr,Ba; $[\text{s-process}/\text{Fe}] = -0.6$ to -0.8). This combination is hard to explain. The atmosphere model they determined was $T_{\text{eff}} = 6000 \pm 150$ K, $\log g = 0.4 \pm 0.4$, and $V_{\text{turb}} = 3.5 \pm 0.5$ km s⁻¹. They also found that it was a high velocity star, with $V_r = -106$ km s⁻¹. On this basis, they concluded that HD 46703 was a low-mass, post-AGB star. Surprisingly, they also found a strong overabundance of sulfur, $[\text{S}/\text{Fe}] = +1.2$, even though the other iron-peak elements had similar abundances to iron (Bond & Luck 1987).

HD 46703 was also shown to be a light variable, with variations peak-to-peak of 0.22 mag over a 12 year period (1966–1979; Luck & Bond 1984) and 0.1 mag over three 1–2 week observing intervals 1981–1982 (Bond et al. 1984). The star was bluer when brighter. On this basis, it was classified as a low-amplitude, semi-regular variable and has been assigned the name V382 Aur.

Waters et al. (1992) included HD 46703 among a small group of post-AGB objects for which they proposed that the selective depletion in the stellar atmosphere arose from the formation of a circumstellar dust disk, in which refractory elements are tied up in the dust and then the volatiles are selectively re-accreted in the atmosphere of the star. Since then, atmospheric depletion patterns have been detected in many more objects (see the recent pa-

pers by Giridhar et al. (2005); Maas, Giridhar, & Lambert (2007); Reyniers & van Winckel (2007) and references therein). Although the process itself is still not well explored theoretically, it seems to be a very common phenomenon among Galactic post-AGB stars as well as in their peers in the LMC.

The original sample of four extremely depleted objects turned out to be binaries (Van Winckel, Waelken 1995) in which there was strong evidence for the presence of a circumbinary disk. Many of the objects subsequently determined to have the chemical depletion anomaly were found to be binaries as well (Van Winckel 2003, and references therein). Using N-band interferometry, Deroo et al. (2006) and Deroo et al. (2007) were able to resolve the disks around some depleted objects, and the main conclusion of their analysis was that the circumstellar disks must be very compact and stable. It is as yet still unclear whether all such depleted stars are binaries surrounded by a circumstellar disk (De Ruyter et al. 2006), or whether there are other circumstances in which depleted photospheres can be formed (Giridhar et al. 2005; Maas, Giridhar, & Lambert 2007).

For large-amplitude pulsators, standard chemical studies based on static atmospheres fall short, and Rao & Reddy (2005) and Giridhar et al. (2005) link the detection of chemical anomalies to a not-well-documented effect in which an anticorrelation between $[X/H]$ and the first ionization potential is created. For pulsational stars with a significant photometric amplitude, any detection of a chemical anomaly should be studied in more detail and preferably using spectra over the whole pulsation cycle.

In this study, we therefore present a study of HD 46703 which combines a detailed chemical study using high-resolution optical spectroscopy with a critical discussion of our photometric and radial velocity monitoring results. This object is an ideal one in which to study in detail the chemical anomalies and to confront those with the pulsational analysis, the nature of the circumstellar material, and the binary connection of the depletion process. The paper is organized as follows: we first analyze the radial velocity to investigate binarity, then the light curves to investigate pulsation, and then the high-resolution spectra to determine the chemical abundance. Finally we discuss the evolutionary nature of the object.

2. RADIAL VELOCITY STUDY

The monitoring of the radial velocity was performed at the Observatoire de Haute-Provence (OHP) from 1989 to 1996 and at the Dominion Astrophysical Observatory (DAO) from 1991 to 1995. The individual velocities are listed in Table 1, where we have included the heliocentric Julian date (HJD), the heliocentric radial velocity (V_r), and the observatory.

Radial velocity data obtained at OHP used the CORAVEL radial velocity meter attached to the 1-m Swiss telescope. CORAVEL is a spectrophotometer by which the radial velocity was obtained by cross-correlations of the stellar spectra with a hardware mask built from the spectrum of the K2 III star Arcturus (Baranne, Mayor, & Poncet 1979). The S/N of the cross-correlation depended therefore also on the spectral match between the science target and Arcturus. The zero-point of the system was regularly assessed during the night by measuring CORAVEL radial velocity standards. This was done at intervals of about 1-2 hours. All the CORAVEL observations, including ours, are held in a data-base that is maintained by the owners of the CORAVELs in the Geneva Observatory (Switzerland).

The observations at the DAO used the 1.2-m telescope equipped with the DAO radial-velocity spectrometer (RVS; McClure et al. 1985; Fletcher et al. 1982) at the Coudé focus. A spectral mask based on the spectrum of Procyon (F5 IV-V) was used, which contained about 340 sharp stellar lines in the wavelength interval from 4000 to 4600 Å. This hardware mask was cross-correlated with the stellar spectrum to determine the radial velocity. A Cd-Ar comparison lamp was observed before and after the stellar observations. These observations were standardized through nightly observations of several radial velocity standard stars (10 on a full night) from the list of Scarfe et al. (1990), which tie the observations very closely to the IAU system (see Scarfe et al. 1990).

It is known that the CORAVEL and DAO–RVS velocities are on very nearly the same standard system, except for a small color term that affects cool stars measured with CORAVEL (Scarfe et al. 1990) and which is not significant for this F star. Therefore we combined the data in the following analysis. This totaled 41 OHP–CORAVEL velocities and 26 DAO–RVS velocities. The precision of the observations is $\pm 0.8 \text{ km s}^{-1}$. We also determined three additional radial velocities from the high-resolution spectra used in Section 5 in the abundance analysis.

These observations show that the object clearly varies in velocity, as shown in Figure 1. The velocities range from -108 to -76 km s^{-1} . They show a periodic pattern of about 600 days, and were fitted with a spectroscopic binary orbit program (Morbey 1975, version from 1986). We also included in the orbital analysis the two earlier radial velocities published by Luck & Bond (1984). Note that the “discordant” low-resolution velocity of $-75 \pm 7 \text{ km s}^{-1}$ from an earlier paper by Bond (1970, see Luck & Bond (1984)) is consistent with one of the extrema of the radial velocity curve. The parameters of the resulting single-lined spectroscopic binary orbit are listed in Table 2. The system has a high velocity of -93.6 km s^{-1} . The orbit is rather eccentric, with a value of $e = 0.31$. The resulting fit of the binary orbit to the radial velocities is shown in Figure 2.

3. LIGHT CURVE STUDY

Photometric observations of HD 46703 were carried out from 1986 through 2006 at three different observatories with two different photometric systems. These are described below.

At the Valparaiso University Observatory (VUO), photometric observations were carried out from 1995 through 2006 using the 0.4-m telescope and CCD camera. In the first several seasons the observations were made primarily with the V filter and occasionally with the R_C , but beginning in 2001 the R_C filter was used regularly. Due to a problem that arose with the V filter, no V data are available from the 1999–2000 through the 2001–2002 observing seasons. The images were reduced using IRAF¹, with normal bias and flat field corrections and using an aperture of diameter 11". Differential magnitudes were obtained between HD 46703 and the comparison star HD 46591 (G0; the same comparison star used by Bond et al. 1984), for which we measured $V = 8.04$ and $(V-R_C) = 0.46$. This comparison star was confirmed to be constant at the level of ± 0.03 mag by comparison with two additional but much fainter stars in the field, and our value of its V magnitude is the same as that reported by Bond et al. (1984). The total number of observations with each filter, and the maximum observational uncertainty, are as follows: 84 with $\sigma \leq \pm 0.007$ mag in V, 48 with $\sigma \leq \pm 0.004$ mag in R_C , and 35 with $\sigma \leq \pm 0.005$ in $(V-R_C)$. Observations of standard stars on several nights were used to transform the differential magnitudes to the standard Johnson V and Cousins R_C systems, and in Table 3 are listed the standardized differential magnitudes. These VUO observations of HD 46703 reveal a variation in brightness over a full range of 0.38 mag in V, with a range of almost that value in 1995–1996 and 2006, and a full range of 0.30 mag in R_C , which is seen in 2006. The $(V-R_C)$ colors shows a variation over a full range of 0.08 mag, reaching 0.07 in 2006, and the system is bluer when brighter.

Observations were also made in the Geneva 7-filter (U,B,V,B1,B2,V1,G) photometric system, both with the 0.7-m Swiss telescope at the Jungfrauoch Observatory and with the 1.2-m Flemish Mercator telescope at the Roque de los Muchachos Observatory at La Palma, Spain. Both telescopes are equipped with a dual-channel photometer that monitored the star and sky quasi-simultaneously, using a filter wheel that cycled through all seven filters four times per second. The photometer at Jungfrauoch is operated manually. The typical uncertainty of an observation is ± 0.005 mag. HD 46703 was observed during two major observing sessions, which resulted in 65 high quality measurements between 1986 Nov and 1996 Jan (3358 d) and 42 measurements between 2001 Oct and 2004 Mar (884 d). These data are listed in Table 4, and they show a peak-to-peak variation of 0.40 mag in the V-band

¹IRAF is distributed by the National Optical Astronomical Observatory, operated by the Association for Universities for Research in Astronomy, Inc., under contract with the National Science Foundation.

with a standard deviation of 0.068 mag.

Since the Geneva V system is essentially identical to the Johnson V system ($\Delta < 0.001$ mag), all of the V data were combined into one set and these are displayed in Figure 3. The data sets show good agreement. Several of the seasons show a clear cyclical pattern, but even within these seasons the amplitude of the variation is not constant. The color variations are typical of pulsations and, as noted previously, the object is bluer when brighter (Figure 4).

Orbital light variations were investigated with the use of the combined V data set. These data were phased with the ephemeris determined for the 600 d orbital period. No significant orbital phase dependence is seen, although, as mentioned above, the light of the system does vary.

4. PULSATIONAL VARIABILITY

The VUO and Geneva photometric data were initially investigated separately for variability, using the CLEAN algorithm based on a Fourier transform (Roberts et al. 1987). The VUO V data suggest a possible period of 29 d and the Geneva V data suggest possible periods of 31 and 27 d, but none of these is very dominant. The analysis of the combined V data yielded two closely spaced periods of 29.06 d and 28.85 d, with the former the stronger. We further investigated the variability using the period analysis program Period04 (Lenz & Breger 2005). This indicates a dominant period of 29.1 d, with the suggestion of amplitude modulation. We also searched for period variability by dividing the data into four separate intervals of 2000 d each. For the second interval, we see a dominant period of 29.1 d, with an amplitude of 0.115 mag. For the third and fourth intervals we find a dominant period of 31.0 d with amplitudes of 0.068 and 0.074 mag, respectively. For the first interval the strongest peak was about 98 d, with an amplitude of 0.054 mag; there was a peak at about 30 d but it was not as strong.

From the complete analysis, we conclude that the system varies with a period of 29.0 d and a varying amplitude, with perhaps a second period of 31 d. Post-AGB stars on the hotter side of the population II Cepheid instability strip often show a very complex pulsational pattern with irregular pulsations (e.g., Kiss et al. 2007). For the limited number of objects with long-term monitoring data, similar, but slightly different periods are found using datasets of different seasons. One of the best studied examples to our knowledge is HD 56126, also a low-metallicity, F spectral type, post-AGB object. The spectroscopic and photometric variations of HD 56126 appear to be consistent with a non-regular radial pulsation where the dominant pulsation mode is the first overtone. In the course of the

pulsation, moderate shock waves are repeatedly generated and they propagate throughout the stellar atmosphere. They provoke a complex, asynchronous motion of the outer layers (Fokin et al. 2001). Similar behavior is found in HD 46703, in which the main period deviates slightly during the different datasets. This exemplifies the complex pulsation character of luminous objects with a small envelope mass.

We searched for a signature of the pulsation in the radial velocities by examining the residuals of the observations compared to the orbital solution. While they vary over a range of 10 km s^{-1} , no periodicity is found in these residuals.

5. CHEMICAL ABUNDANCE STUDY

High resolution, high signal-to-noise optical spectra were obtained with the (now de-commissioned) Utrecht Echelle Spectrograph (UES) mounted on the 4.2-m William Herschel Telescope (WHT) on La Palma, Spain. The echelle with $31.6 \text{ lines mm}^{-1}$ was used, and the projected slit width was $1.1''$ on the sky, yielding a resolution of $R \simeq 50,000$. The spectra were taken in February 1994 with a few nights separation (Feb 21, 23 and 28), in three different settings to cover the whole optical region (364–1022 nm with spectral gaps from 665 nm redwards). These UES spectra were kindly provided by Dr. Eric Bakker and used by him in his analysis of the optical circumstellar molecular absorption bands (Bakker et al. 1997). Two sample regions of the spectrum are displayed in Figure 5, with the same spectral region of a bright star (HR 1017 or HR 1865) and of AC Her shown for comparison. HR 1017 is an F5 Iab star ($B-V=0.45$) and HR 1865 is an F0 Ib star ($B-V=0.22$), both with solar composition, while AC Her ($B-V=0.63$) is a post-AGB object with chemical anomalies (Van Winckel et al. 1998) similar to HD 46703. In Figure 5a is shown the spectral region around $\lambda 6150 \text{ \AA}$, displaying a number of lines of FeI, FeII, BaII, and the OI triplet. The weakness of the iron lines in HD 46703 compared to those in HR 1865 is readily apparent. In Figure 5b is shown the spectral region around the Zn line $\lambda 4810.54 \text{ \AA}$. The difference in strength of the Zn line relative to the other metal lines in HD 46703 compared to HR 1017 can easily be seen. The spectrum of HD 46703 has a S/N ratio of ~ 200 in the red but is less in the blue.

The general analysis methodology is already extensively discussed in many of our previous papers (e.g., Reyniers et al. 2004; Deroo et al. 2005) and will not be described in detail. We performed an LTE abundance study and determined the fundamental parameters of the photosphere in an iterative scheme. We first estimated the temperature (using a given gravity and metallicity) by requiring the abundances to be independent of the excitation level. The gravity was then fine-tuned by requiring ionization balance for all species for

which lines of different ions could be identified. The microturbulence was quantified by requiring the abundances to be independent of line strength. Finally, we iterated this scheme so that convergence was found for all fundamental parameters. We note that we used the latest ATLAS models (Castelli & Kurucz 2004) in combination with the latest version (April 2002) of Sneden’s LTE line analysis program MOOG (Sneden 1973). The model atmosphere parameters were inferred from a detailed model study based on the iron lines. The final parameters were found to be as follows: an effective temperature of $T_{\text{eff}} = 6250 \pm 250$ K, a gravity of $\log g = 1.0 \pm 0.05$, a microturbulent velocity of $V_t = 3.0 \pm 1.0$ km s⁻¹, and a model metallicity of $[M/H] = -1.5$.

The abundance measurements derived from the individual lines of each ion are listed in Table 5. Listed for every line are the wavelength, the excitation potential (χ), the $\log gf$ value, the measured equivalent width (W_λ), the absolute abundance ($\log \epsilon = \log(N(X)/N(H)) + 12$), and the abundance difference between the individual line and the mean abundance ($\Delta \log \epsilon$).

A summary of the abundances is listed in Table 6. The first column of this table gives the ion, the second column gives the number of lines used, the third one is the mean equivalent width of the lines used, the fourth column gives mean absolute abundances derived, the fifth column is the line-to-line scatter (σ_{tl}) in $\log \epsilon$, and the sixth column gives the abundance relative to the Sun $[X/H]$. The solar abundances (seventh column) are needed to calculate the $[X/H]$ values (for references, see Reyniers et al. 2007). The dust condensation temperatures listed (eighth column) are those given by Lodders (2003, and references therein). They are computed using a solar abundance mix at a pressure of 10^{-4} atm. A condensation temperature for O is meaningless, since O is the most abundant element in rock material.

The abundances are also presented graphically in Figure 6, where the abundances relative to solar $[X/H]$ are plotted against condensation temperature. The clear anti-correlation as seen in Figure 6 can immediately be recognized as a depletion pattern; elements with a low condensation temperature, like S, Zn and the CNO-elements, have a much higher photospheric abundance than elements with a high (>1000 K) condensation temperature. The CNO elements have low condensation temperatures and are typically expected not to be depleted. The low carbon abundance of $[C/H] = -0.3$ makes it clear that HD 46703 has not experienced a third dredge-up. Also, the lack of an overabundance of the s-process elements relative to the elements with the same condensation temperature supports that conclusion. The $[Zn/Fe\text{-peak}]$ and $[S/Ti]$ ratios are diagnostics for depletion, since they are elements with the same chemical history, but with different condensation temperatures. For this object, these element ratios are $[Zn/Fe] = +0.82$ and $[S/Ti] = +1.04$, indicating that a very efficient depletion process took place.

Our new results can be compared with the abundance analysis of this source published

by Luck & Bond (1984) more than twenty years ago. The spectra for their study date from 1976, 1980 and 1981, and therefore reflect the status of the spectroscopic technology of that time: the signal-to-noise ratio of their spectra is rather low (as can be seen on their Fig. 3). While the authors derive abundances for a large number of elements, the line-to-line scatter is fairly high (typically around 0.4 dex, while ours is ≤ 0.2 dex). Besides the inferior quality of their data (compared to current standards), this large scatter may also be attributed to the fact that their analysis is based on spectra taken on different dates over several years (and hence different pulsational phases), whereas our spectra were obtained over a shorter interval of seven days. Nevertheless, the abundances that are in common in both analyses are in good agreement. Due to the large line-to-line scatter, however, the depletion pattern is far less clear from the Luck & Bond (1984) abundances. Their Zn abundance is only moderately overabundant compared to iron ($[\text{Zn}/\text{Fe}] = +0.2$), and they do not list an S abundance. The iron abundance they derive is $[\text{Fe}/\text{H}] = -1.56$, ~ 0.2 dex higher than ours, which is due to their slightly cooler model (6000 K). Their model atmosphere parameters ($T_{\text{eff}} = 6000$ K, $\log g = 0.4$, $V_t = 3.5$ km s $^{-1}$) are, however, consistent with ours to within the errors. In a later paper (Bond & Luck 1987), the same authors derive nitrogen and sulphur abundances based on a new spectrum and obtained $[\text{N}/\text{H}] = +0.22$ and $[\text{S}/\text{H}] = -0.34$; their $[\text{N}/\text{H}]$ value is similar to our value but their $[\text{S}/\text{H}]$ value is higher than ours by +0.36.

Luck & Bond (1984) made a special remark on the H α line, which showed narrow blue and red emission peaks that rise to the level of the continuum and that vary slightly between their two spectra (their Figure 3). The H α that we observe is similar, with the blue and red emission components having equal strengths.

6. DISCUSSION

HD 46703 has a high velocity (at galactic latitude $+20^\circ$), a low gravity, and a low carbon abundance, all of which point to it being an evolved, low-mass, post-AGB star. The chemical depletion pattern indicates the presence of a circumbinary disk, for which there is also evidence from the observed intrinsic polarization (Trammell et al. 1994). The depletion of Fe and other Fe-peak elements make the estimate of the initial metallicity difficult. Assuming the photospheric Zn abundance was not affected by photospheric depletion, the initial metallicity was about -1.0 .

De Ruyter et al. (2006) present a systematic spectral energy distribution study of post-AGB stars around which disks are suspected. This whole sample is a significant fraction of all known post-AGB stars in the Galaxy (e.g., Szczerba et al. 2007). Recently we found similar objects in the Large Magellanic Cloud (e.g., Reyniers & van Winckel 2007). HD 46703

is among the minority of this disk sample that show no clear signature of a near-IR excess (De Ruyter et al. 2006, Figure A.1.). In most cases, dust is present at the sublimation temperature, which is not the case in HD 46703. This suggests a larger disk radius. Nonetheless, the disk is likely only resolvable by interferometric means (Deroo et al. 2007).

HD 46703 is by no means the only disk post-AGB star for which the binary orbit is determined (e.g., Van Winckel 2007, and references therein). One of the surprising results of all the orbital studies so far is the fact that many objects survived their phase of strong binary interaction in rather wide orbits. Moreover, many systems, like HD 46703, are eccentric, despite the fact that tidal effects as well as orbital-energy dissipation (during a likely common envelope phase) are expected to rapidly circularize the orbits. Episodic mass loss caused by periastron mass transfer in an elliptic orbit has been proposed as a main mechanism (Soker 2000; Bonačić Marinović et al. 2008), but also disk-binary interactions may be strong enough to pump the eccentricity (Artymowicz et al. 1991). The latter mechanism is only efficient when the dust extends outward to a distance of only a few times the major axis of the orbit. For HD 46703, the lack of a near-IR excess points to the lack of dust at the sublimation radius and thus a larger disk radius. Orbital pumping by the actual disk is not likely the main eccentricity pumping mechanism for HD 46703.

The global picture that emerges of all those objects is that a binary star evolved in a system that is (presently) too small to accommodate a full grown AGB star. During a badly understood phase of strong interaction, a circumbinary dusty disk was formed, but the binary system did not suffer a dramatic spiral in. What we observe now is an F–K supergiant in a binary system that is surrounded by a circumbinary dusty disk in a bound orbit. Understanding the evolution of the disks, as well as their impact on the evolution of the central stars, become important challenges in the study of the final evolution of a significant fraction of binary stars.

We thank W. Zima for help with the period analysis using Period04, and we acknowledge the observing contribution of many undergraduate research students at Valparaiso University. BJH acknowledges financial support from the National Science Foundation (9018032, 0407087), and MR acknowledges financial support from the Fund for Scientific Research - Flanders (Belgium).

REFERENCES

Artymowicz, P., Clarke, C.J., Lubow, S.H., & Pringle, J.E. 1991, *ApJ*, 370, L35

- Bakker, E. J., van Dishoeck, E. F., Waters, L. B. F. M., & Schoenmaker, T. 1997, *A&A*, 323, 469
- Baranne, A., Mayor, M., & Poncet, J. L. 1979, *Vistas in Astronomy*, 23, 279
- Bonačić Marinović, A.A., Glebbeek, E., & Pols, O.R. 2008, *A&A*, 480, 797
- Bond, H.E. 1970, *ApJS*, 22, 17
- Bond, H.E., Carney, B.W., & Grauer, A. 1984, *PASP*, 96, 176
- Bond, H.E., & Luck, R.E. 1987, *ApJ*, 312, 203
- Castelli, F. & Kurucz, R. L. 2004, astro-ph/0405087
- Deroo, P., Acke, B., Verhoelst, T., Dominik, C., Tatulli, E., & van Winckel, H. 2007, *A&A*, 474, L45
- Deroo, P., Reyniers, M., Van Winckel, H., Goriely, S., & Siess, L. 2005, *A&A*, 438, 987
- Deroo, P., van Winckel, H., Min, M., et al. 2006, *A&A*, 450, 181
- De Ruyter, S. 2005, PhD thesis, KU Leuven
- De Ruyter, S., van Winckel, H., Maas, T., Lloyd Evans, T., Waters, L. B. F. M., & Dejonghe, H. 2006, *A&A*, 448, 641
- Fletcher, J. M., Harris, H. C., McClure, R. D., & Scarfe, C. D. 1982, *PASP*, 94, 1017
- Fokin, A. B., Lèbre, A., Le Coroller, H., & Gillet, D. 2001, *A&A*, 378, 546
- Giridhar, S., Lambert, D. L., Reddy, B. E., Gonzalez, G., & Yong, D. 2005, *ApJ*, 627, 432
- Kiss, L. L., Derekas, A., Szabó, Gy. M., Bedding, T. R., & Szabados, L. 2007, *MNRAS*, 375, 1338
- Lenz, P., & Breger, M. 2005, *Co. Ast.*, 146, 53
- Lodders, K. 2003, *ApJ*, 591, 1220
- Luck, R.E., & Bond, H.E. 1984, *ApJ*, 279, 729
- Maas, T., Giridhar, S., & Lambert, D.L. 2007, *ApJ*, 666, 378

- McClure, R. D., Fletcher, J.M., Grundmann, W. A., & Richardson, E. H. 1985, in IAU Col. 88: Stellar Radial Velocities, ed. A.G.D. Phillip & D.W. Latham (Schenectady: L. Davis Press), 49
- Morbey, C.L. 1975, PASP, 87, 689
- Rao, K., & Reddy, B. E. 2005, Bul. Astron. Soc. India, 33, 374
- Reyniers, M., Abia, C., van Winckel, H., Lloyd Evans, T., Decin, L., Eriksson, K., & Pollard, K. R. 2007, A&A, 461, 641
- Reyniers, M., & van Winckel, H. 2007, A&A, 463, L1
- Reyniers, M., Van Winckel, H., Gallino, R., & Straniero, O. 2004, A&A, 417, 269
- Roberts, D.H., Lehár, J., & Dreher, J.W. 1987, AJ, 93, 968
- Scarfe, C. D., Batten, A. H., & Fletcher, J. M. 1990, Publ. Dom. Astr. Obs., 28, 21
- Snedden, C. A. 1973, Ph.D. Thesis, University of Texas at Austin
- Soker, N. 2000, A&A, 357, 557
- Szczerba, R., Siódmiak, N., Stanskińska, G. & Borkowski, J. 2007, A&A, 469, 799
- Trammell, S.R., Dinerstein, H.L., & Goodrich, R.W. 1994, AJ, 108, 984
- Van Winckel, H. 2003, ARA&A, 41, 391
- Van Winckel, H. 2007, Baltic Astronomy, 16, 112
- Van Winckel, H., Waelkens, C., & Waters, L. B. F. M. 1995, A&A, 293, L25
- Van Winckel, H., Waelkens, C., Waters, L. B. F. M., Molster, F. J., Udry, S., & Bakker, E. J. 1998, A&A, 336, L17
- Waters, L.B.F.M., Trams, N.R., & Waelkens, C. 1992, A&A, 262, L37

Table 1. List of Radial Velocity Observations of HD 46703

HJD	V_r (km s^{-1})	Obs ^a	HJD	V_r (km s^{-1})	Obs ^a	HJD	V_r (km s^{-1})	Obs ^a
2443054.6670	-106.20	1	2448663.3810	-93.52	2	2449239.9700	-96.14	3
2443055.6670	-105.00	1	2448714.7852	-88.53	3	2449244.0167	-91.57	3
2447757.6570	-105.75	2	2448714.8364	-87.27	3	2449244.0291	-92.37	3
2447758.6500	-100.31	2	2448719.7471	-84.59	3	2449264.0109	-93.04	3
2447760.6490	-101.17	2	2448725.3480	-84.27	2	2449287.0101	-92.04	3
2447761.6500	-103.66	2	2448726.3280	-84.24	2	2449384.7473	-78.52	3
2447945.4130	-103.14	2	2448727.3420	-85.20	2	2449405.4097	-77.9	4
2447961.3080	-102.22	2	2448728.3270	-85.49	2	2449406.5792	-77.9	4
2447972.3380	-98.28	2	2448730.3570	-84.71	2	2449411.5368	-77.0	4
2447975.4080	-99.81	2	2448731.3400	-86.08	2	2449575.6330	-107.11	2
2447977.3510	-100.92	2	2448733.7322	-86.07	3	2449576.6290	-109.95	2
2447996.3940	-97.51	2	2448736.7225	-85.83	3	2449577.6350	-108.66	2
2447997.3380	-97.49	2	2448756.7085	-83.32	3	2449580.6260	-106.59	2
2447998.3730	-97.09	2	2448769.7557	-78.46	3	2449800.7381	-98.24	3
2448000.3580	-99.62	2	2448778.7807	-79.70	3	2449955.6550	-82.23	2
2448348.3360	-97.39	2	2448875.9727	-79.29	3	2450020.9430	-75.68	3
2448353.3460	-98.88	2	2448922.8683	-88.88	3	2450101.4540	-83.96	2
2448354.3560	-100.51	2	2448952.8581	-98.07	3	2450122.3620	-86.99	2
2448531.0476	-105.83	3	2449084.3400	-105.82	2	2450142.3580	-99.70	2
2448531.9238	-107.71	3	2449086.3630	-106.58	2	2450178.3600	-100.56	2
2448566.8739	-99.52	3	2449089.3400	-105.47	2	2450208.3400	-104.77	2
2448600.8751	-97.18	3	2449130.7615	-104.27	3	2450232.3860	-109.33	2
2448627.8152	-99.24	3	2449196.6340	-100.20	2	2450293.6190	-107.46	2
2448628.8664	-97.95	3	2449201.6230	-103.17	2	2450295.6170	-106.64	2

^aReferences for the velocities: (1) Luck & Bond (1984), where we have estimated the fractional JD based on the observing data and location; (2) OHP–CORAVEL; (3) DAO–RVS; (4) derived from our high-resolution spectra used for the abundance analysis.

Table 2. Orbital Solution of HD 46703

Parameter (units)	Value	σ
V_o (km s ⁻¹)	-93.65	0.28
K_1 (km s ⁻¹)	16.85	0.54
e	0.323	0.023
Ω	1.194	0.090
T_o	2448907.991	7.358
Period (day)	599.88	1.26
σ (km s ⁻¹)	2.04	...
$a \sin i$ (AU)	0.879	0.029
$f(M)$ (M_\odot)	0.252	0.025

Table 3. Differential Magnitudes of HD 46703 from VUO^a

HJD - 2,400,000	ΔV	HJD - 2,400,000	ΔR_C
49,793.6586	1.030	49,951.9198	1.039
49,802.6261	1.068	50,169.6203	1.306
49,827.6171	1.062	50,184.6021	1.047
49,840.5517	0.845	50,191.6014	1.064
49,951.9178	0.873	50,385.7577	1.093
49,965.8989	1.055	51,257.6332	1.137
49,987.8408	0.903	51,882.7167	1.086
50,001.8460	1.009	51,937.6837	1.087

^aTable 3 is published in its entirety in the electronic edition of the *Astronomical Journal*. A portion is shown here for guidance regarding form and content.

Table 4. Magnitudes of HD 46703 on the Geneva Seven-Filter System^{a,b}

HJD - 2,400,000	U	B	V	B1	B2	V1	G
46,742.605	10.652	8.753	9.067	9.735	10.136	9.799	10.117
46,762.609	10.523	8.592	8.973	9.549	9.994	9.704	10.033
46,765.555	10.502	8.555	8.943	9.506	9.961	9.676	10.005
46,768.542	10.492	8.585	8.953	9.539	9.980	9.684	10.016
46,775.473	10.514	8.630	9.000	9.577	10.027	9.739	10.059
46,804.360	10.543	8.611	8.984	9.576	10.014	9.725	10.051
46,814.350	10.661	8.736	9.077	9.719	10.153	9.838	10.164
46,815.400	10.636	8.728	9.063	9.696	10.119	9.791	10.113

^aTable 4 is published in its entirety in the electronic edition of the *Astronomical Journal*. A portion is shown here for guidance regarding form and content.

^bObservations from 2446742–2450101 were made with the Swiss 0.7-m telescope and from 2452205–2453090 with the Flemish 1.2 Mercator telescope.

Table 5. Measurements of the individual lines of each ion used in the abundance analysis of HD 46703.^{a,b}

λ (Å)	χ (eV)	$\log gf$	W_λ (mÅ)	$\log \epsilon$	$\Delta \log \epsilon$
Abundance Results for C I					
4228.33	7.68	-2.250	49	8.26	0.00
4371.37	7.65	-1.970	80	8.31	0.05
4770.03	7.46	-2.330	48	8.15	-0.11
4771.74	7.46	-1.757	105	8.20	-0.06
4775.90	7.49	-2.194	60	8.18	-0.08
4817.37	7.48	-2.889	27	8.40	0.14
5017.09	7.95	-2.431	21	8.21	-0.05
5023.85	7.95	-2.196	22	8.00	-0.26
5039.06	7.95	-1.775	94	8.53	0.27
5040.13	7.95	-2.301	18	8.00	-0.26

^aTable 5 is published in its entirety in the electronic edition of the *Astronomical Journal*. A portion is shown here for guidance regarding form and content.

^bThe following model atmosphere was adopted: $T_{\text{eff}} = 6250$ K, $\log g = 1.0$, $V_t = 3.0$ km s⁻¹, and $[M/H] = -1.5$.

Table 6. Summary of the abundance results for HD 46703.^a

Ion	N	\overline{W}_λ (mÅ)	$\log \epsilon$	σ_{tot}	[X/H]	$\log \epsilon_\odot$	T_{cond} (K)
C I	23	62	8.26	0.15	−0.31	8.57	40
N I	5	46	8.16	0.14	+0.17	7.99	123
O I	3	22	8.37	0.20	−0.49	8.86	...
Na I	2	21	4.96	0.13	−1.37	6.33	958
Mg I	5	49	6.05	0.22	−1.49	7.54	1336
Al I	2	155	4.45	0.14	−2.02	6.47	1653
Si I	1	11	6.10	...	−1.44	7.54	1310
Si II	3	56	6.24	0.17	−1.30	7.54	1310
S I	4	22	6.63	0.15	−0.70	7.33	664
Ca I	18	37	4.78	0.18	−1.58	6.36	1517
Sc II	7	44	1.10	0.16	−2.07	3.17	1659
Ti II	31	49	3.23	0.16	−1.79	5.02	1582
Cr I	6	80	3.75	0.24	−1.92	5.67	1296
Cr II	16	56	4.11	0.18	−1.56	5.67	1296
Mn I	2	21	3.59	0.15	−1.80	5.39	1158
Fe I	106	44	5.78	0.16	−1.73	7.51	1334
Fe II	29	52	5.77	0.14	−1.74	7.51	1334
Ni I	6	22	4.67	0.18	−1.58	6.25	1353
Zn I	3	40	3.68	0.14	−0.92	4.60	726
Y II	4	37	0.38	0.07	−1.86	2.24	1659
Zr II	2	16	0.94	0.14	−1.66	2.60	1741
Ba II	4	80	0.66	0.13	−1.47	2.13	1455

^aThe following model atmosphere was adopted: $T_{\text{eff}} = 6250$ K, $\log g = 1.0$, $V_t = 3.0$ km s^{−1}, and $[M/H] = -1.5$.

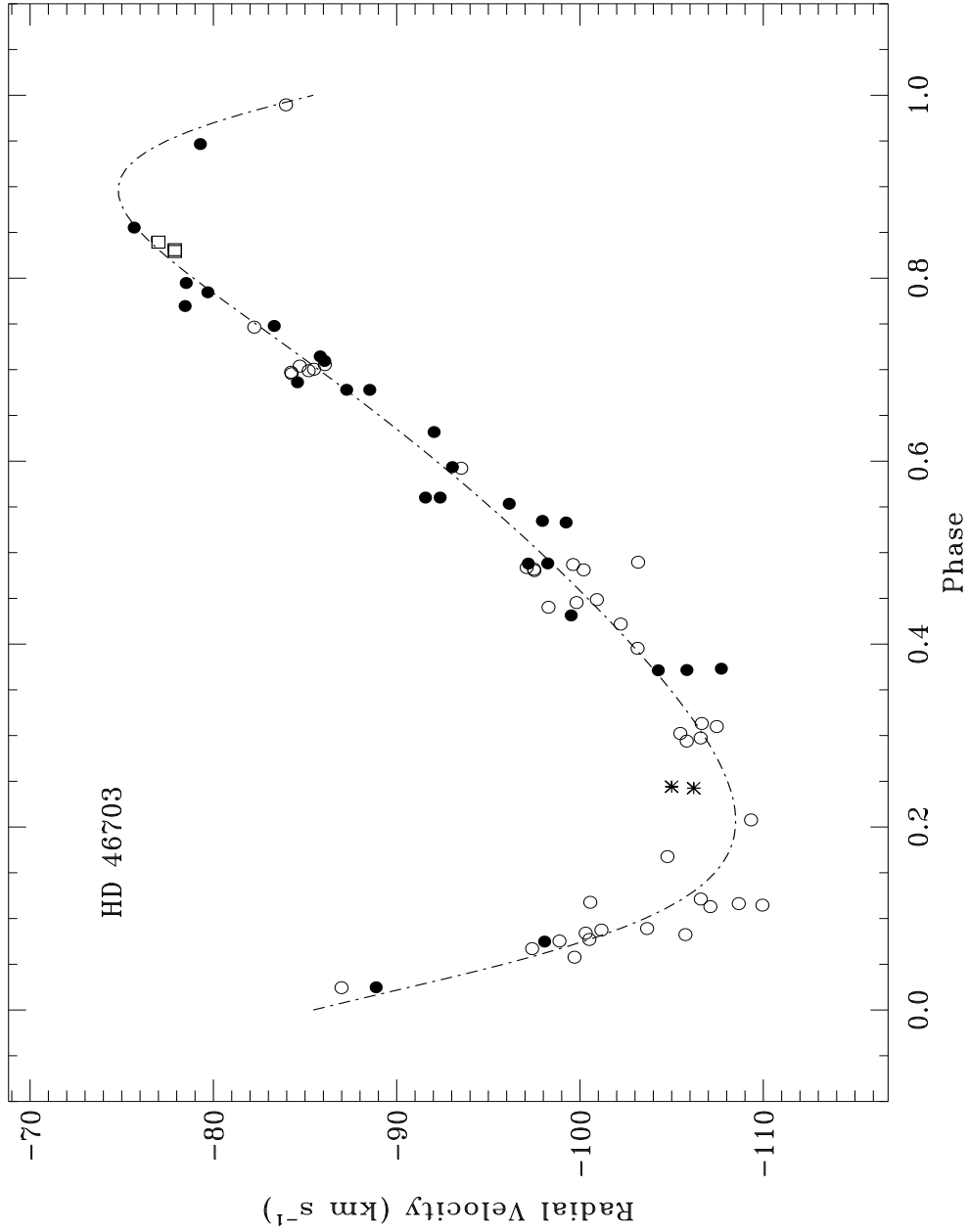


Fig. 2.— Phase plot of velocities of HD 46703 fit with the binary orbit parameters of Table 2. The symbols are the same as in Figure 1, with the additional two velocities of Luck & Bond (1984) shown as asterisks.

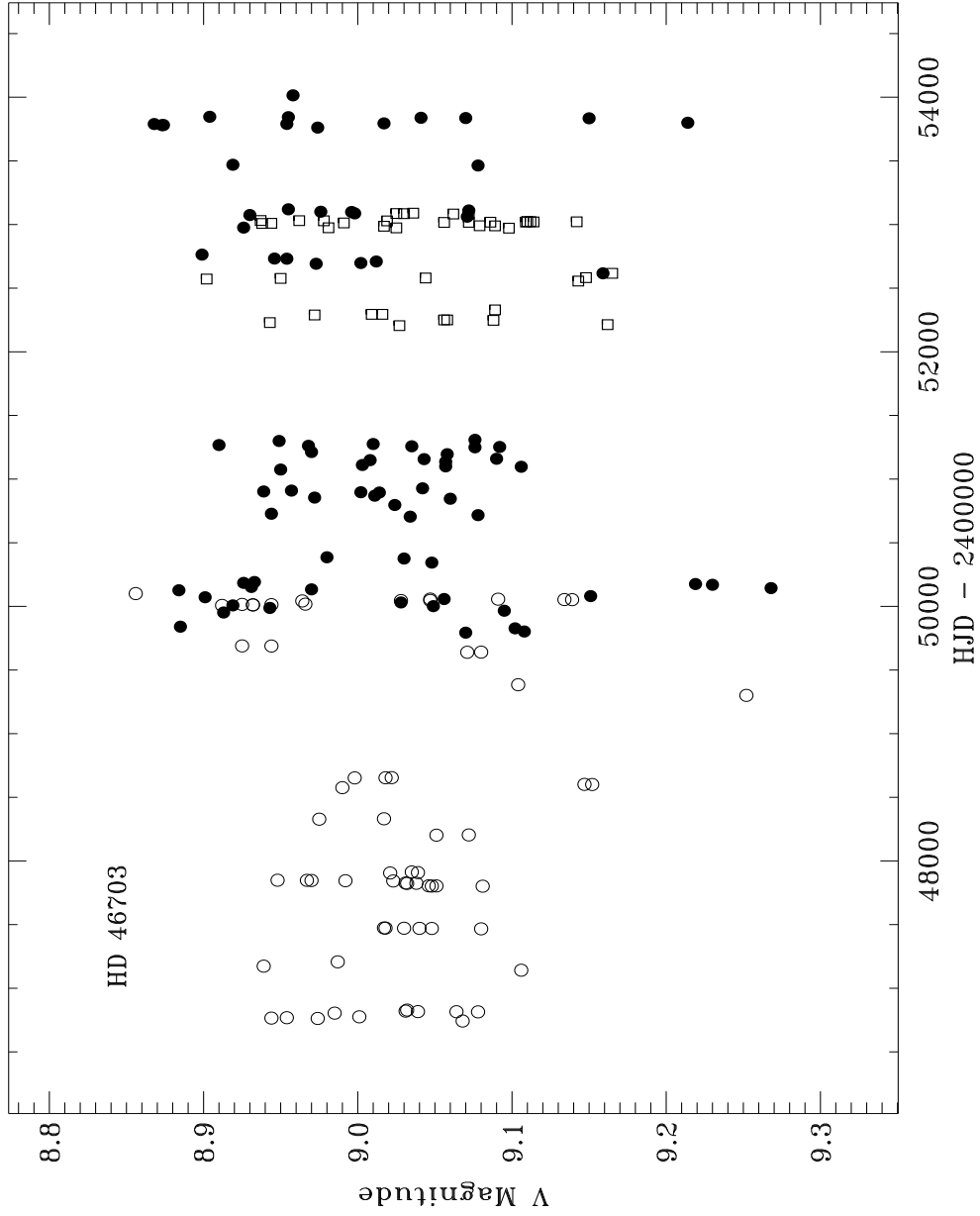


Fig. 3.— V light curve HD 46703 from 1986 to 2006. The symbols are as follows: open circle - Swiss telescope at Jungfraujoch, filled circle - VUO telescope, open square - Mercator telescope at La Palma.

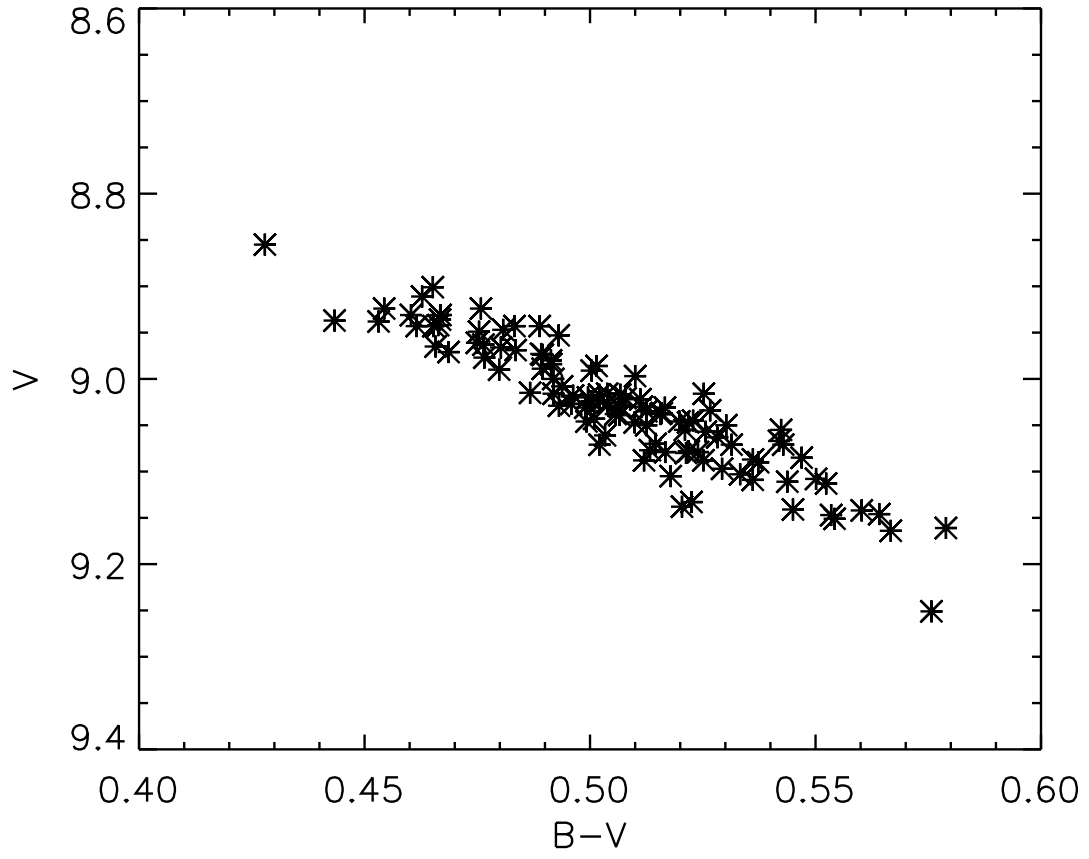


Fig. 4.— Color-magnitude plot for HD 46703, based on the Geneva photometry transformed to the Johnson system. The system is bluer when brighter.

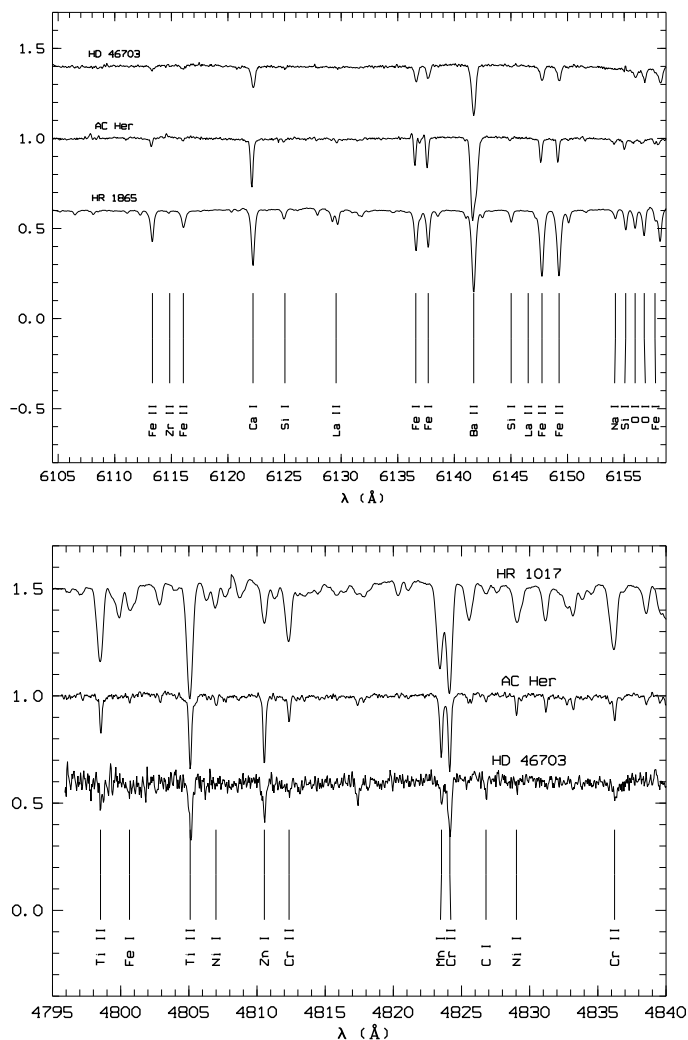


Fig. 5.— Plots of sample regions of the spectrum of HD 46703. (a) Top — The region around $\lambda 6150$ Å. The weakness of the Fe lines in HD 46703 relative to those in HR 1865 (F0 Ib, solar composition) is readily seen. (b) Bottom — The region around the Zn line $\lambda 4810.54$ Å. Note the difference in strength of the Zn line relative to the other metal lines in HD 46703 compared with HR 1017 (F5 Iab, solar composition). Also shown for comparison is the post-AGB object AC Her (metal-poor, similar depletion pattern).

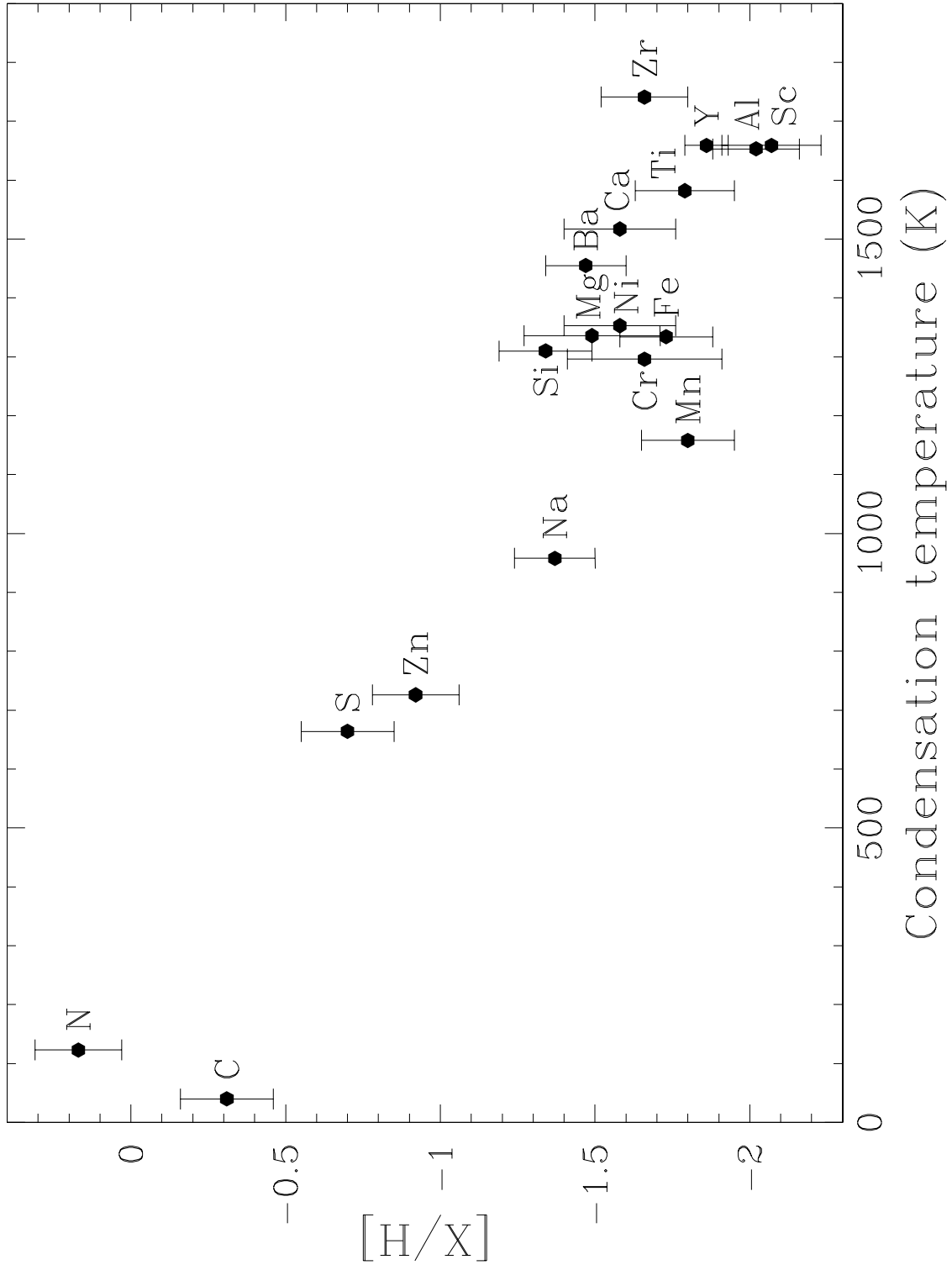


Fig. 6.— Abundance results for HD 46703. The anti-correlation of abundance with condensation temperature clearly indicates a depletion effect.